J Neurophysiol 94: 3023–3036, 2005.
First published July 13, 2005; doi:10.1152/jn.00002.2005.

Vibratory Adaptation of Cutaneous Mechanoreceptive Afferents

S. J. Bensmaïa,[1,2] Y. Y. Leung,[3] S. S. Hsiao,[1,2,3] and K. O. Johnson[1,2,3]
[1]*Krieger Mind/Brain Institute, and* [2]*Departments of Neuroscience and* [3]*Biomedical Engineering, Johns Hopkins University, Baltimore, Maryland*

Submitted 3 January 2005; accepted in final form 11 July 2005

Bensmaïa, S. J., Y. Y. Leung, S. S. Hsiao, and K. O. Johnson. Vibratory adaptation of cutaneous mechanoreceptive afferents. *J Neurophysiol* 94: 3023–3036, 2005. First published July 13, 2005; doi:10.1152/jn.00002.2005. The objective of this study was to investigate the effects of extended suprathreshold vibratory stimulation on the sensitivity of slowly adapting type 1 (SA1), rapidly adapting (RA), and Pacinian (PC) afferents. To that end, an algorithm was developed to track afferent absolute (I_0) and entrainment (I_1) thresholds as they change over time. We recorded afferent responses to periliminal vibratory test stimuli, which were interleaved with intense vibratory conditioning stimuli during the adaptation period of each experimental run. From these measurements, the algorithm allowed us to infer changes in the afferents' sensitivity. We investigated the stimulus parameters that affect adaptation by assessing the degree to which adaptation depends on the amplitude and frequency of the adapting stimulus. For all three afferent types, I_0 and I_1 increased with increasing adaptation frequency and amplitude. The degree of adaptation seems to be independent of the firing rate evoked in the afferent by the conditioning stimulus. In the analysis, we distinguished between additive adaptation (in which I_0 and I_1 shift equally) and multiplicative effects (in which the ratio I_1/I_0 remains constant). RA threshold shifts are almost perfectly additive. SA1 threshold shifts are close to additive and far from multiplicative (I_1 threshold shifts are twice the I_0 shifts). PC shifts are more difficult to classify. We used an integrate-and-fire model to study the possible neural mechanisms. A change in transducer gain predicts a multiplicative change in I_0 and I_1 and is thus ruled out as a mechanism underlying SA1 and RA adaptation. A change in the resting action potential threshold predicts equal, additive change in I_0 and I_1 and thus accounts well for RA adaptation. A change in the degree of refractoriness during the relative refractory period predicts an additional change in I_1 such as that observed for SA1 fibers. We infer that adaptation is caused by an increase in spiking thresholds produced by ion flow through transducer channels in the receptor membrane. In a companion paper, we describe the time-course of vibratory adaptation and recovery for SA1, RA, and PC fibers.

INTRODUCTION

Extended exposure to a suprathreshold vibratory stimulus applied to the skin results in a reversible decrement in vibratory sensitivity. This desensitization—known as vibratory or vibrotactile adaptation—has been characterized in psychophysical experiments either as an increase in threshold (Capraro et al. 1979; Gescheider and Wright 1968; Gescheider et al. 1979; Hahn 1968a,b, 1966; Hollins et al. 1990, 1996; Verrillo and Gescheider 1977) or as a reduction in the perceived intensity of a suprathreshold stimulus (Berglund and Berglund 1970; Gescheider and Wright 1969; Hahn 1968b, 1966). The degree of desensitization produced by a given adapting stimulus depends on its amplitude and frequency (Capraro et al. 1979; Gescheider et al. 1979; Hollins et al. 1990; Verrillo and Gescheider 1977). The adapting efficacy of a vibratory adapting stimulus can be predicted from its ability to stimulate one of two populations of mechanoreceptors and their central connections (Gescheider et al. 1979; Verrillo and Gescheider 1977). Low-frequency vibration primarily excites the rapidly adapting (RA) and slowly adapting type I (SA1) systems, which terminates in Meissner corpuscles and Merkel receptors and results in a selective reduction in the sensitivity to low-frequency vibratory stimuli. High-frequency vibration primarily excites the Pacinian (PC) system, which terminates in Pacinian corpuscles and results in a selective reduction in the sensitivity to high-frequency vibratory stimuli. The function of adaptation may be to adjust the dynamic range of the perceptual system to enhance its ability to acquire information about the environment (Keidel et al. 1961). Vibrotactile adaptation has been shown, under certain conditions, to enhance subjects' ability to discriminate vibratory stimuli based on amplitude (Delemos and Hollins 1996; Goble and Hollins 1993) and frequency (Goble and Hollins 1994).

The evidence suggests that vibrotactile adaptation occurs both centrally (O'Mara et al. 1988; Whitsel et al. 2003), and—as we report here and in a companion paper (Leung et al. 2005)—at the periphery. O'Mara et al. (1988) found the effects of adaptation to be less pronounced and its dynamics slower at the periphery than at higher perceptual stages and proposed that adaptation is caused by ionic changes in the extracellular environment of central neurons or their afferent terminals. Similarly, Whitsel et al. (2000) found the responses of RA afferents to decrease only slightly during intense vibratory stimulation, whereas those of RA cortical neurons exhibited a steep decline (Whitsel et al. 2003). They hypothesized that adaptation results from short-term temporal dynamics in networks of neurons in SI cortex (Lee and Whitsel 1992; Lee et al. 1992).

The challenge in measuring neural adaptation is to devise a method for tracking sensitivity as it changes over time. Impulse frequency evoked by an unchanging stimulus has been used as the index of sensitivity in the aforementioned neurophysiological studies investigating vibrotactile adaptation (O'Mara et al. 1988; Whitsel et al. 2000, 2003). Spike rate provides a useful index of changes in sensitivity only if impulse rate is a strictly monotonic function of vibratory intensity. In fact, impulse rates in mechanoreceptive afferents rise monotonically only within a limited range of amplitudes. Over much of the intensity range, RA and PC afferents are either silent (at intensities less than the absolute threshold) or they fire exactly once per cycle (within the so-called tuning or entrainment plateau) (Freeman and

Address for reprint requests and other correspondence: S. J. Bensmaia, Krieger Mind/Brain Inst., Johns Hopkins Univ., 3400 N. Charles St, Krieger Hall 338, Baltimore, MD 21218 (E-mail: sliman@jhu.edu).

The costs of publication of this article were defrayed in part by the payment of page charges. The article must therefore be hereby marked "*advertisement*" in accordance with 18 U.S.C. Section 1734 solely to indicate this fact.

Johnson 1982a; Johnson 1974; Talbot et al. 1968). When stimulus amplitude is below the absolute threshold or within the entrainment plateau, changes in sensitivity do not result in changes in spike rate (see Fig. 1).

We developed a method for tracking the sensitivity of SA1, RA, and PC afferents before, during, and after the presentation of adapting stimuli of various amplitudes, frequencies, and durations. Because the firing rates of these afferents are described by a stereotyped, piecewise linear function of vibratory intensity (Fig. 1) defined by I_0 (the minimum amplitude evoking any response) and I_1 (the minimum amplitude evoking 1 impulse on every cycle), I_0 and I_1 are well suited to track the instantaneous changes in afferent fiber responsivity (Freeman and Johnson 1982a; Johnson 1974). In this paper, we characterize the frequency and amplitude dependence of threshold shifts for SA1, RA, and PC fibers and compare the properties of afferent adaptation to those of psychophysical adaptation. We then discuss possible mechanisms of afferent adaptation.

METHODS

All experimental protocols complied with the guidelines of the Johns Hopkins University Animal Care and Use Committee and the NIH Guide for the Care and Use of Laboratory Animals. Single-unit recordings were made from the ulnar and median nerves of five Macaque monkeys (*Macaca mulatta*) using standard methods (Talbot et al. 1968). Standard procedures were used to classify the mechanoreceptive afferents according to their responses to step indentations and vibratory stimulation (Freeman and Johnson 1982a,b; Talbot et al. 1968). An afferent was classified as SA1 if it produced sustained firing in response to a step indentation. It was classified as RA if it had a small receptive field and responded only to the onset and offset of an indentation. It was classified as PC if *1*) it was vigorously activated by air blown gently over the hand; *2*) it was activated by transmitted vibrations produced by tapping on the hand restraint; and *3*) its receptive field was large. The point of maximum sensitivity of the afferent was located on the skin using Von Frey monofilaments and marked with a felt-point pen.

The stimulator consisted of a feedback-controlled linear motor (Chubbuck 1966) that drove a 1-mm-diam probe. A three-dimensional translation stage was used to position the probe so that its motion was normal to the skin surface. The probe was glued to the skin at the point of maximum sensitivity with cyanoacrylate glue and vibrated around the resting position of the skin to ensure *1*) that SA1 afferents were not excited by static preindentation and *2*) that the probe maintained contact with the skin throughout stimulation.

Each stimulus run consisted of a preadaptation period, an adaptation period, and a recovery period. Test stimuli, 1 s long, were presented every 4 s. The 3-s interstimulus interval (ISI) was empty during the preadaptation and recovery periods and was filled with the adapting stimulus during the adaptation period. Figure 2 shows the structure of a stimulus run.

The amplitude and frequency of the adapting stimulus, the frequency of the test stimuli, the duration of the adaptation period, and the duration of the recovery period varied from run to run. Adapting and test frequencies were selected to maximally excite afferents of each class: For SA1 afferents, the test and adapting frequencies were 10, 30, and 60 Hz in every possible pair; for RA afferents, test and adapting frequencies were 30, 60, and 100 Hz; for PC afferents, frequencies of 60, 100, 200, and 300 Hz were used. Adapting amplitudes ranged from 1 to 25 times the unadapted absolute threshold (I_0) (reported amplitudes are 0-to-peak micrometers). Adaptation periods lasted 1, 2, 4, 8, or 16 min. Recovery continued until I_0 and I_1 returned to preadaptation values.

Because recording times were limited, individual afferents were not tested under all combinations of adapting amplitude, adapting frequency, and test frequency. Instead, experimental blocks were designed so that one stimulus parameter varied between runs while the other parameters remained constant. A subset of all possible series was run on each fiber.

A tracking algorithm, described in detail in the Appendix, was used to estimate each fiber's I_0 and I_1 on every trial. Because SA1, RA, and PC impulse rates evoked by vibratory stimuli are piecewise linear functions of vibratory intensity, I_0 and I_1 characterize each fiber's rate-intensity function over a wide range of intensities (Fig. 1) (Freeman and Johnson 1982a; Johnson 1974). Preadaptation, adapted, and recovered thresholds were estimated using the means of the last five (absolute and entrainment) threshold measurements in each period. The degree of adaptation, or threshold shift, produced by a given

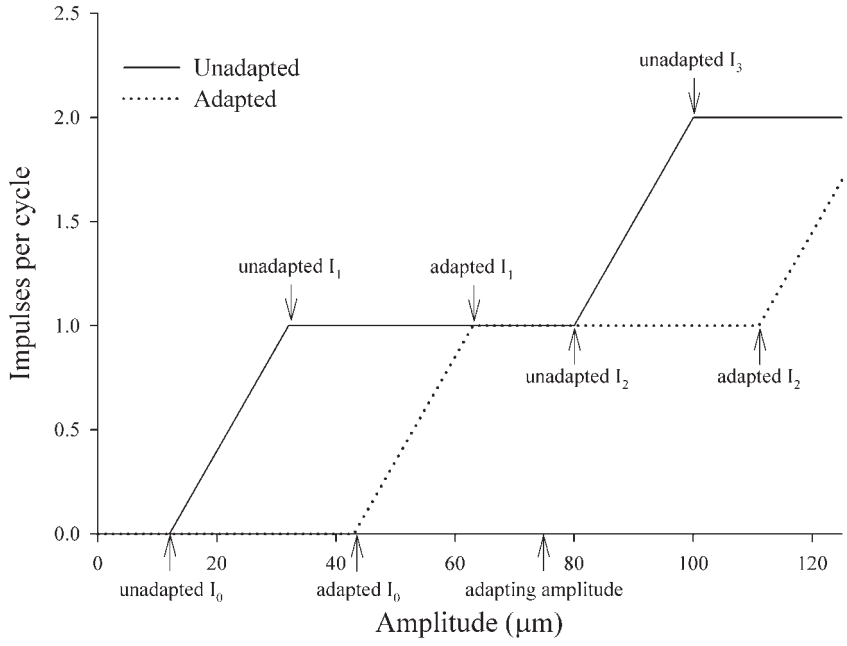

FIG. 1. Impulse rates in slowly adapting 1 (SA1) rapidly adapting (RA) and Pacinian (PC) afferents evoked by vibratory stimuli. Because the relationship between impulse rate and vibratory amplitude is piecewise linear with broad plateaus in all 3 afferent types, the entire function is defined by thresholds for each linear segment. I_0 denotes the absolute threshold (minimum amplitude that evokes a response), I_1 the entrainment threshold (minimum amplitude that evokes a single action potential on each vibratory cycle), I_2 the doubling threshold (minimum amplitude that evokes 2 impulses on some stimulus cycles), and I_3 the double entrainment threshold (minimum amplitude that evokes 2 impulses on every stimulus cycle) (Johnson 1974). The problem with using impulse rate as an index of adaptation is shown by the hypothetical example shown here, in which a 75-μm stimulus amplitude would evoke the same (entrained) impulse rate throughout the adaptation and recovery periods despite the fact that I_0 tripled over that period.

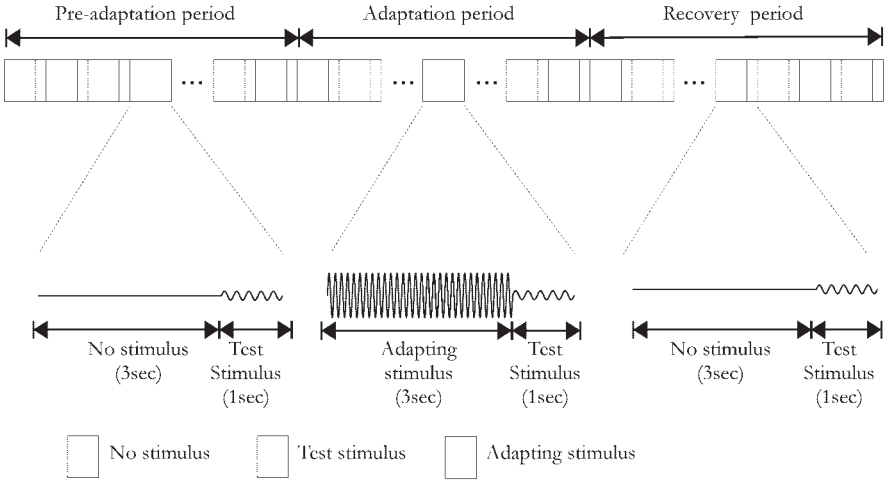

FIG. 2. Time-course of an experimental run. Each run is divided into 3 periods: preadaptation, adaptation, and recovery period. Each trial comprises a 4-s interval consisting of a 3-s interval, which is empty except during the adaptation period followed by a 1-s test stimulus. Adaptation and recovery periods were 1, 2, 4, 8, or 16 min long. The preadaptation period, whose only purpose was to establish the unadapted I_0 and I_1 thresholds, was about 1 min long.

adapting stimulus was specified as the difference between adapted and unadapted thresholds. The effects of adaptation reached steady state within the adaptation period for all afferents (Leung et al. 2005).

RESULTS

Results obtained from 9 SA1, 11 RA, and 11 PC fibers are reported here.

Unadapted thresholds

Absolute and entrainment thresholds, I_0 and I_1, measured in the preadaptation period conform to those obtained in previous studies (Freeman and Johnson 1982a; Talbot et al. 1968): SA1 fibers tended to have the highest, RA fibers intermediate, and PC fibers the lowest thresholds (Fig. 3). The typical U-shaped threshold curve was observed for PC fibers, whereas SA1 and

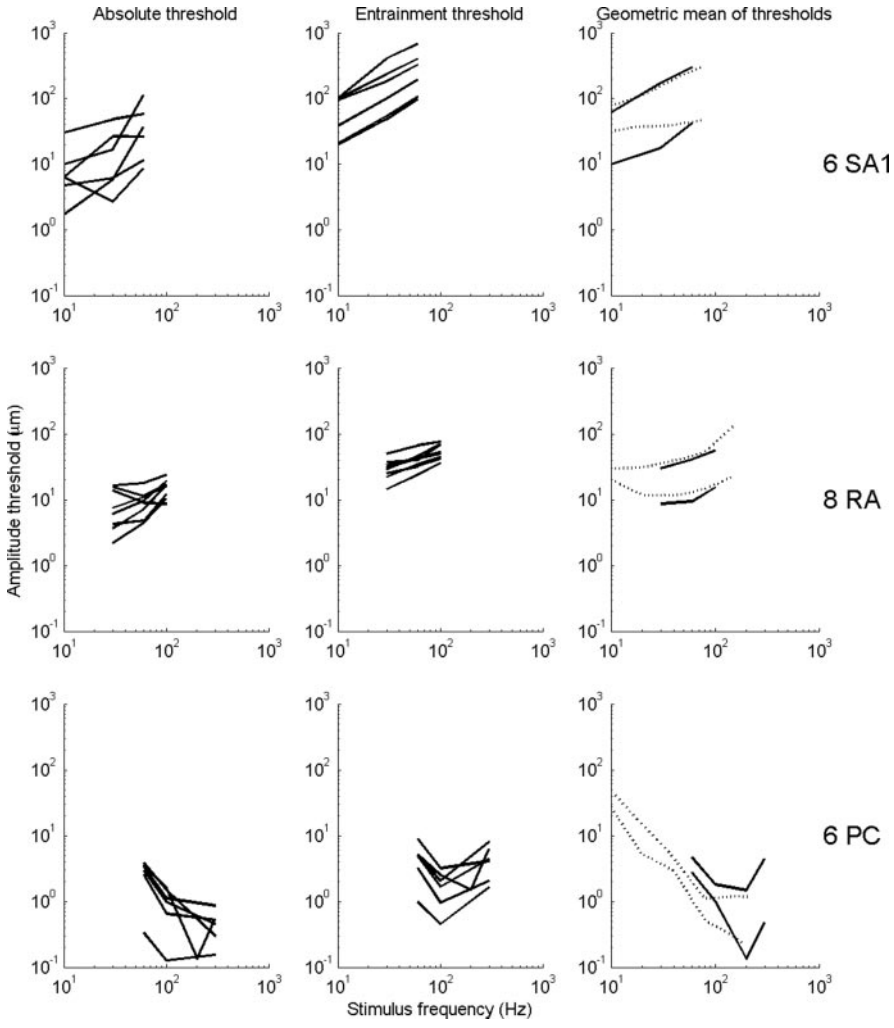

FIG. 3. Absolute and entrainment thresholds. Thresholds obtained from a given afferent are included in the plot only if they were measured at 3 or more frequencies. Dotted lines in the 3rd column denote absolute and entrainment thresholds measured by Freeman and Johnson (1982a).

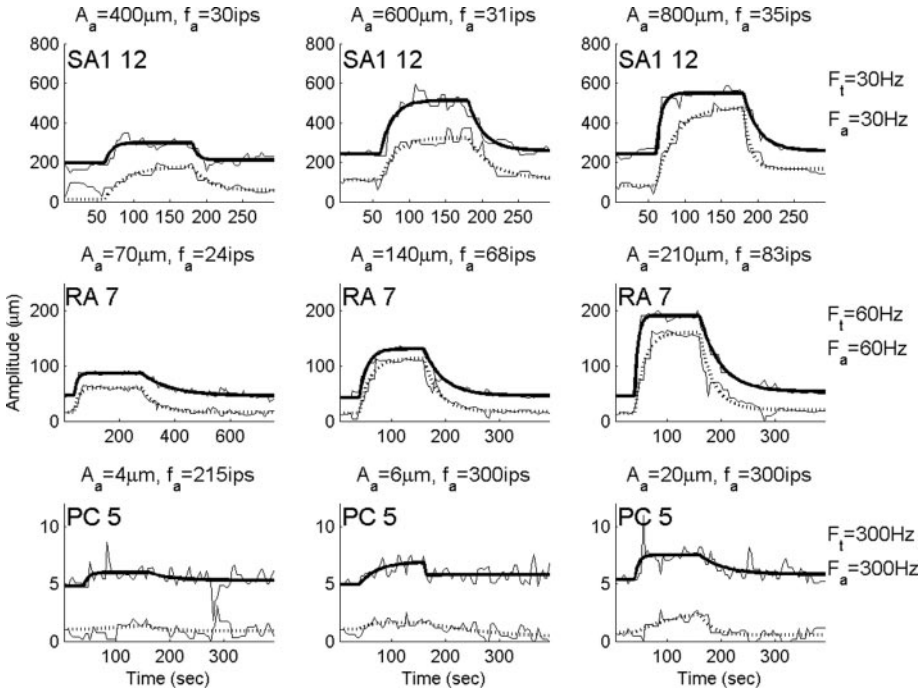

FIG. 4. Time-course of adaptation and recovery for 1 afferent of each type at 3 adapting amplitudes. Each plot shows the absolute and entrainment threshold amplitudes as they change over time. Data obtained during adaptation and recovery periods are fit with exponential, functions (Leung et al. 2005). Dotted lines, I_0; thick solid lines, I_1; A_a, adapting amplitude; f_a, spike rate evoked in the afferent by the adapting stimulus; F_t, test frequency; F_a, adapting frequency. Stimulus and response parameters that vary from run to run are listed at the *top* of each plot. Constant stimulus parameters are listed at the *right* of each row.

RA thresholds increased with frequency over the range at which they were tested.

Effects of adapting amplitude

Figure 4 shows, for one fiber of each type, the general finding that absolute and entrainment thresholds rose exponentially during the adaptation period. Furthermore, the asymptotic level to which thresholds rose increased monotonically with increasing adaptation amplitude. Finally, it can be seen from the figure that SA1 and RA fibers tended to be more susceptible to adaptation than PC fibers. As shown in Figs. 5–7 for typical afferents of each type, the relationship between threshold shift and adapting amplitude was approximately linear within the range of amplitudes tested. Median slopes of the functions relating the shift in I_0 to adapting amplitude were 0.15, 0.32, and 0.018 for SA1, RA, and PC fibers (median correlation coefficients: 0.90, 0.96, and 0.72, respectively). The corresponding values for I_1 were 0.25, 0.36, and 0.04 (median correlation coefficients: 0.91, 0.97, and 0.92, respectively). PC fibers were much less susceptible to adaptation than were SA1 and RA afferents, even when threshold shifts and adapting amplitudes were expressed as ratios of absolute threshold (DISCUSSION). Also, the shift in I_1 tended to be greater than that in I_0 for SA1 and PC fibers but not for RA afferents.

Effects of adapting frequency

Figure 8 shows, for one typical fiber of each type, that the degree of adaptation was affected by the frequency of the

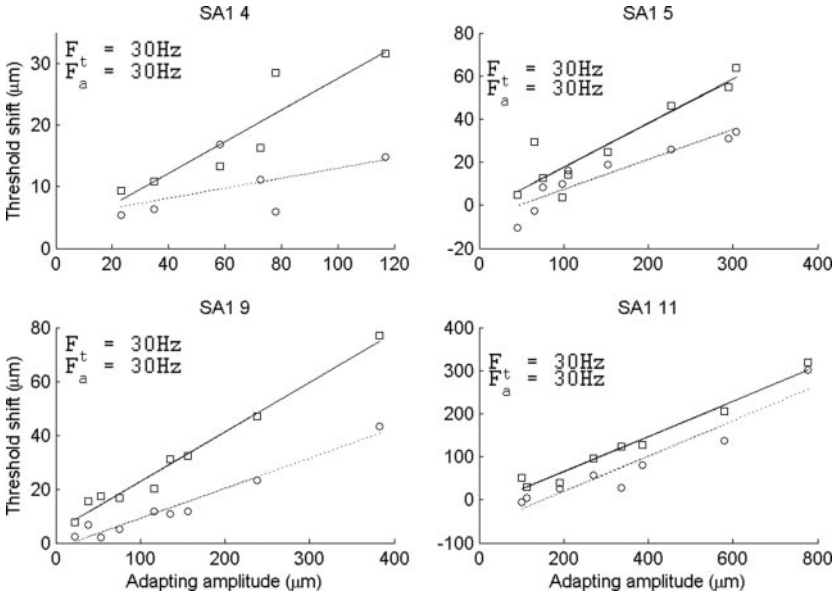

FIG. 5. Effects of adapting amplitude on threshold shift for 4 typical SA1 afferents. Circles and dotted line, absolute thresholds; squares and solid line, entrainment thresholds.

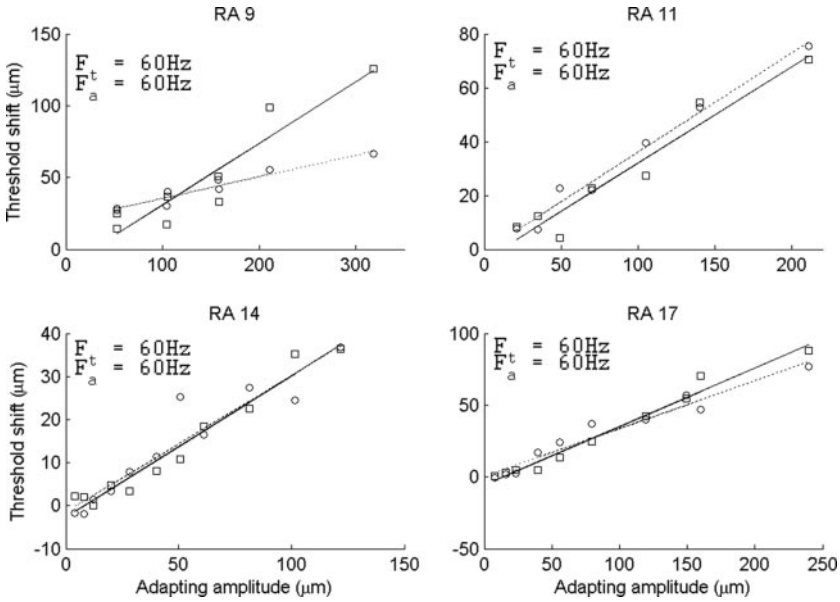

FIG. 6. Effects of adapting amplitude on threshold shift for 4 RA afferents. Convention as in Fig. 5.

adapting stimulus when test frequency and adapting amplitude were held constant. For all three afferents, the degree of adaptation increased as the frequency of the adaptor increased, even though the adapting amplitudes remained constant. For instance, the entrainment threshold of the SA1 fiber increased from 60 to 140 μm as the adapting frequency increased from 10 to 60 Hz. The *top three panels* of Fig. 9 show threshold shift—averaged across test frequencies and adapting amplitudes—as a function of adapting frequency for each class of fibers. For all three afferent types, thresholds rose substantially with increasing adapting frequency when test frequency and adapting amplitude were held constant. This result was unexpected as SA1 and RA thresholds actually rose with increasing vibratory frequency, indicating a decline in sensitivity (Fig. 3). A simple prediction from the threshold frequency function of SA1 and RA fibers is that a vibratory stimulus of constant amplitude would decline in effective intensity with increasing frequency and thus have a declining effect on adaptation. The increase in adapting effectiveness indicates that some other aspect of increasing frequency is important.

Effects of adaptor-elicited firing rate

A strong possibility, based on the data shown in Fig. 9, is that adaptation depends on firing rate, because both the firing rate evoked by the adaptor and threshold shift increased, on average, with adapting frequency. However, careful examination of the effects of adaptation amplitude on firing rate and threshold shift show that this is not the case. For instance, the mean firing rate evoked by the adapting stimulus in the SA1 fiber shown in Fig. 4 increased only from 30 to 35 impulses per second (ips) as the amplitude of the adapting stimulus increased from 400 to 800 μm, yet I_0 and I_1 both increased by ~300 μm. Figure 10 shows examples in which threshold shift rose substantially as adapting amplitude increased despite the fact that the mean impulse rate evoked by the adapting stimulus

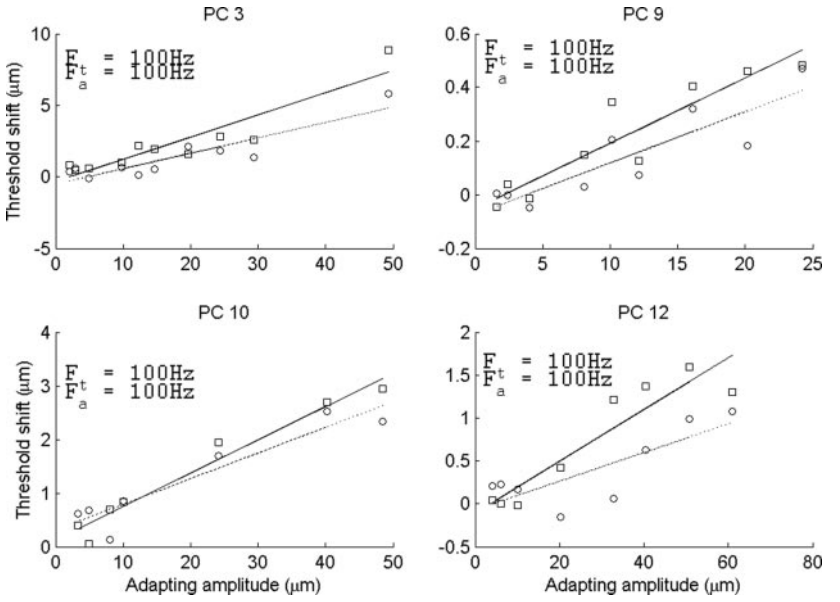

FIG. 7. Effects of adapting amplitude on threshold shift for 4 PC afferents. Conventions as in Fig. 5.

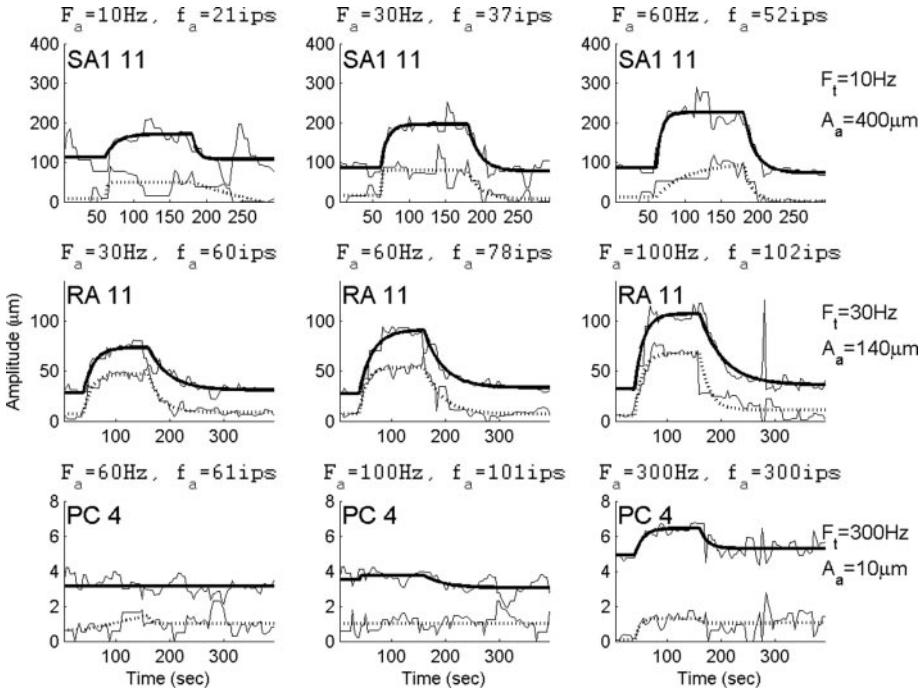

FIG. 8. Time-course of adaptation and recovery for 1 afferent of each type at 3 adapting frequencies. Conventions as in Fig. 4.

was unchanged. Such an increase in threshold shift without a concomitant increase in adaptor-evoked spike rate was observed in six SA1, nine RA, and seven PC fibers (67% of the SA1 fibers, 81 % of the RA fibers, and 64% of the PC fibers from which measurements were derived). In many cases, the firing rate remained constant over large changes in adapting amplitude (e.g., a 10 to 1 change in amplitude for the PC fiber in Fig. 10) because of the broad entrainment plateau (the wide range of amplitudes that produce 1 impulse per stimulus cycle). For the RA shown in Fig. 10, for example, the shifts in I_0 and I_1 double as the adapting amplitude doubles while the spike rate remains constant and entrained to the 60-Hz stimulus. Figure 11 shows the threshold shifts produced in an SA1 fiber by a set of nine adapting stimuli: Six of the stimuli entrain the

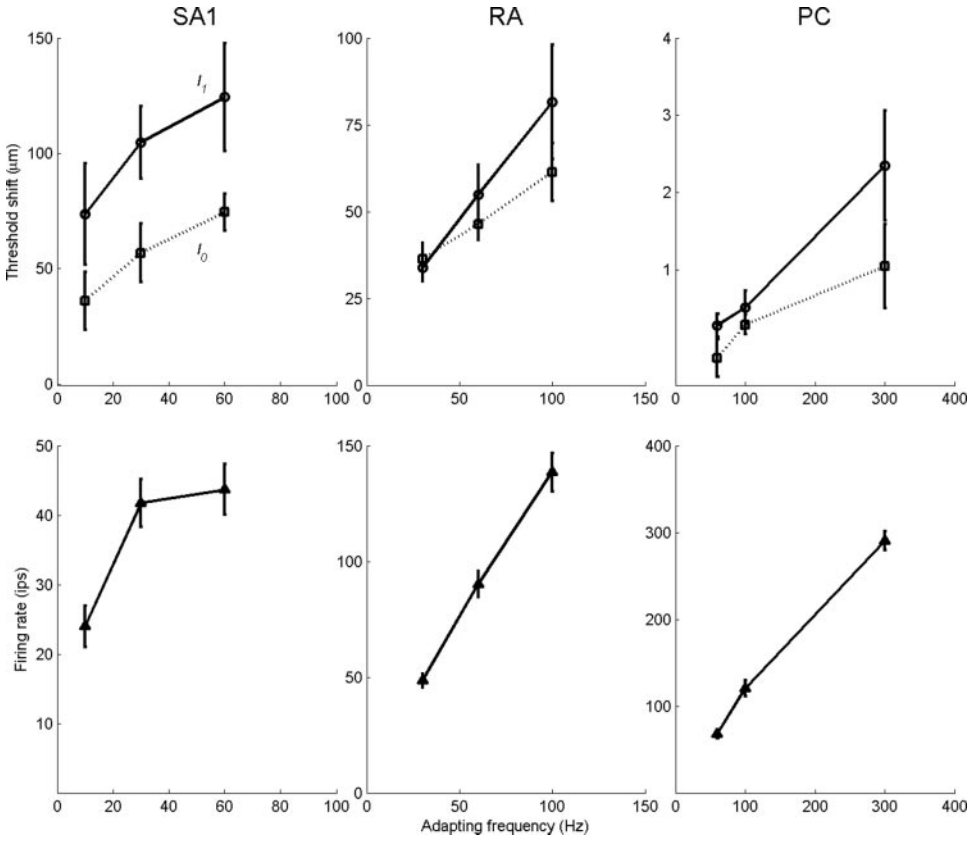

FIG. 9. Effect of adapting frequency on mean threshold shift and on adaptor evoked firing rate. In the *top panels,* squares and dotted lines denote absolute thresholds; circles and solid lines denote entrainment thresholds. Error bars denote SE (these are inflated as effects of frequency are collapsed across amplitudes). Only cases in which all 3 adapting frequencies were combined with a single adapting amplitude were included. *Bottom panels:* mean spike rate evoked in afferents at each adapting frequency (error bars denote SE ($N_{SA1} = 9, N_{RA} = 11, N_{PC} = 11$).

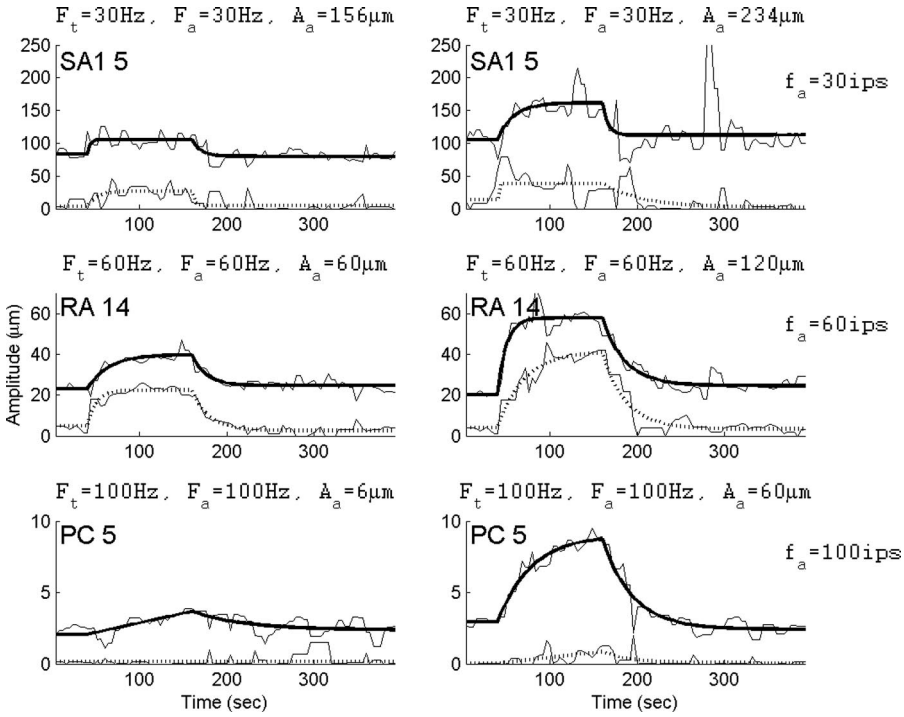

FIG. 10. Examples in which adapting amplitudes and adaptation varied widely but evoked action potential rates remained constant. Conventions as in Fig. 4.

afferent but produce threshold shifts that span an order of magnitude. Because large increments in threshold shift can be produced without changes in firing rate, it is evident that factors other than firing rate play a major role in adaptation.

To assess quantitatively whether firing rate contributes to adaptation, we regressed threshold shift on both adaptor-evoked firing rate and stimulus amplitude when test and adapting frequency were held constant. If adaptation can be explained in terms of adapting amplitude and is independent of firing rate, slopes relating threshold shift to firing rate should be approximately zero. On the other hand, if firing rate contributes to adaptation, the function relating threshold shift to adapting amplitude should be steeper when increments in amplitude produce increments in spike rate than when they do not (as would be the case if the increased adapting amplitude remains within the entrainment plateau). According to this scenario, regression coefficients for firing rate should be positive. In the five cases (4 RA and 1 SA[1]) in which there were enough observations to obtain statistically reliable regression coefficients for both rate and adapting amplitude (with test and adapting frequency constant), the coefficient for spike rate was not significantly different from zero, while that for amplitude was significantly positive.[1] This analysis supports the hypothesis that threshold shift is independent of spike rate because *1*) increments in threshold shift are observed in the absence of increases in adaptor-evoked spike rate and *2*) threshold shifts are not larger when both adapting amplitude and spike rate increase than when only amplitude increases.

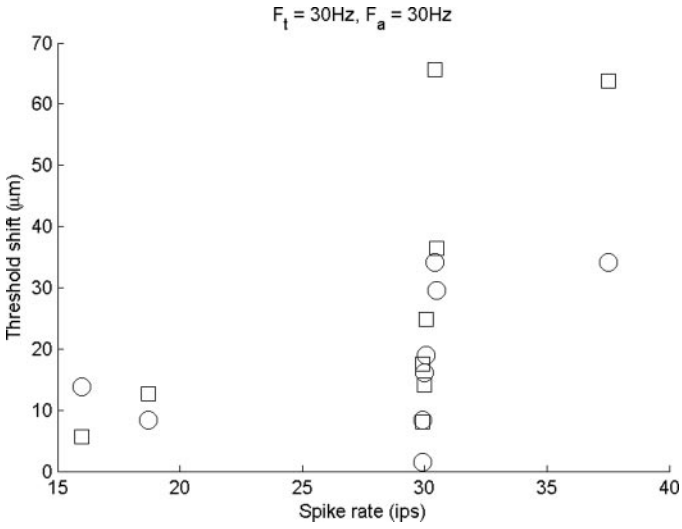

FIG. 11. Shift in absolute (circles) and entrainment (squares) threshold vs. adaptor-elicited firing rate for 1 SA1 afferent (SA 2). Test and adapting frequencies were 30 Hz, and adapting amplitudes varied from 75 to 300 μm. Six of the 9 adapting stimuli evoked similar spike rates but produced shifts in I_0 and I_1 that span an order of magnitude.

Comparing the effects of adaptation on I_0 and I_1

The relative effects of adaptation on I_0 and I_1 may provide clues as to the mechanisms underlying adaptation. For example, a change in the gain of the mechanoelectrical transducer

[1] We also performed an analysis of covariance (ANCOVA) on threshold shift with spike rate and amplitude as covariates (including a random factor to partial out differences across neurons of a given type), pooling data obtained at all adapting and test frequencies. We found that the effect of amplitude was highly significant for both types of thresholds in all three types of afferents ($P < 0.01$), while that of spike rate was significant in only one case: the change in the I_0 of RA afferents. The problem with this analysis is that it does not take into account the spectral sensitivity profile of the afferents (i.e., the fact that afferents are more sensitive at some vibratory frequencies than others). It is noteworthy that the only significant effect of firing rate was found for RA afferents. Indeed, for the four RA afferents for which we had sufficient data to perform the analysis, we found no effect of spike rate on threshold shift beyond that accounted for by amplitude, when test and adapting frequency were held constant. Thus the effect of spike rate on ΔI_0 observed in the ANCOVA is likely because of the differential sensitivity of RA afferents to adapting stimuli that vary in frequency.

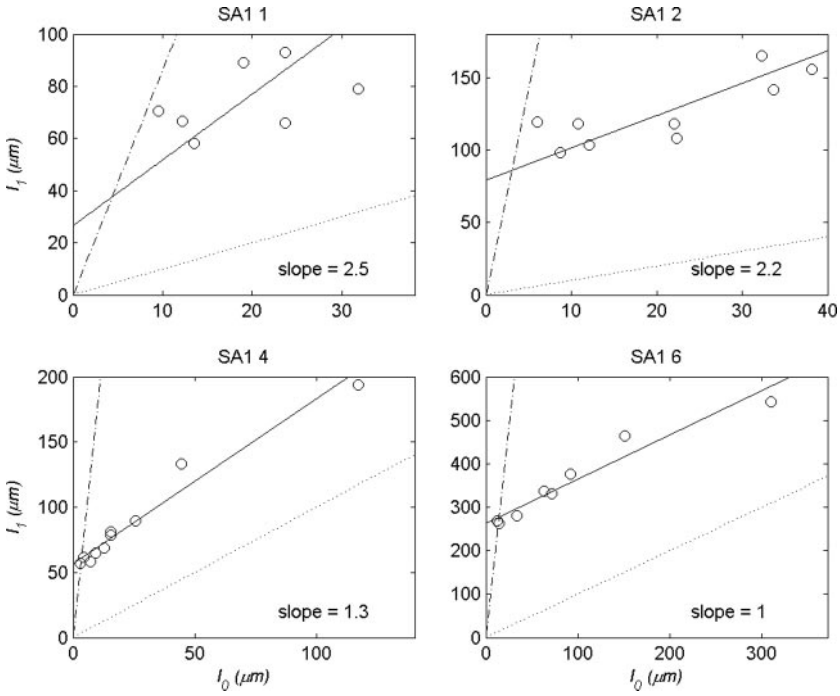

FIG. 12. I_1 vs. I_0 after SA1 adaptation. Dotted lines correspond to the line with unit slope, $I_1 = I_0$, dashed lines show the relationship expected when I_0 and I_1, change multiplicatively during adaptation (i.e., the ratio I_1 II_0 = *constant*). Solid line is the regression line through the final, adapted I_0, I_1 pairs corresponding to different adaptation amplitudes. Slope in the *bottom right corner* of each graph is the regression slope. A regression line with a slope near 1.0 indicates that the shifts in I_0 and I_1 were additive (and nearly identical). Two of the 4 SA1 afferents had substantially larger shifts in I_1 than I_0 but none came close to a multiplicative change in I_0 and I_1 which would require that the regression coincide with the dashed line.

mechanisms (e.g., a progressive inactivation of mechanosensitive ion channels) would shift I_0 and I_1 by the same multiplicative factor. On the other hand, a change in the threshold for action potential production might manifest itself as equal, additive shifts in I_0 and I_1 (DISCUSSION). Because shifts in I_0 and I_1 tend to be linearly related (Figs. 12–14), the slope of the function relating I_1 to I_0 constitutes an index of the additivity or multiplicativity in the shifts. A slope of one indicates additive, equal increments dI_0 and dI_1. A slope equal to the initial, unadapted I_1/I_0 ratio indicates a multiplicative effect. For SA1 and RA afferents, multiplicative and additive slopes tend to be considerably different and the actual slopes point to additive rather than multiplicative effects (Figs. 12 and 13). For PC afferents, the multiplicative slopes are much closer to one (because unadapted I_1/I_0 ratios in PCs tend to be close to 1), which makes it difficult to distinguish between additive and multiplicative changes (Fig. 14).

A population analysis is shown in Fig. 15, which shows the initial I_1/I_0 ratios and the slopes relating dI_1 to dI_0 (*left column*). For all of the afferents, the modal slope relating dI_1 to dI_0 is near one. Virtually all RA afferents have slopes close to one whereas more SA1 and PC fibers have slopes of two or

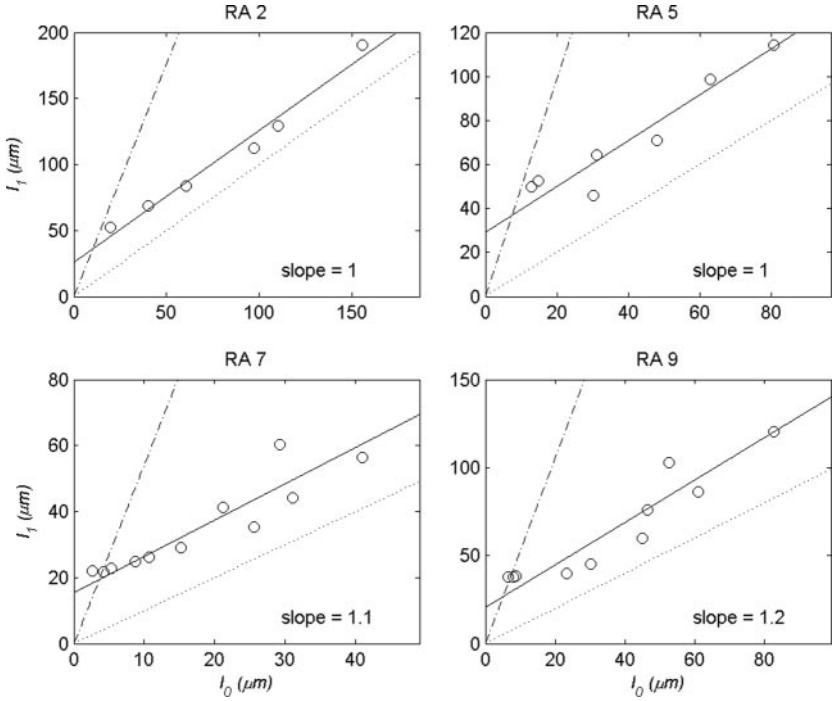

FIG. 13. I_1 vs. I_0 after RA adaptation. Conventions as in FIG. 12. Note that in every fiber the shifts in I_0 and I_1 are additive and identical (or nearly so).

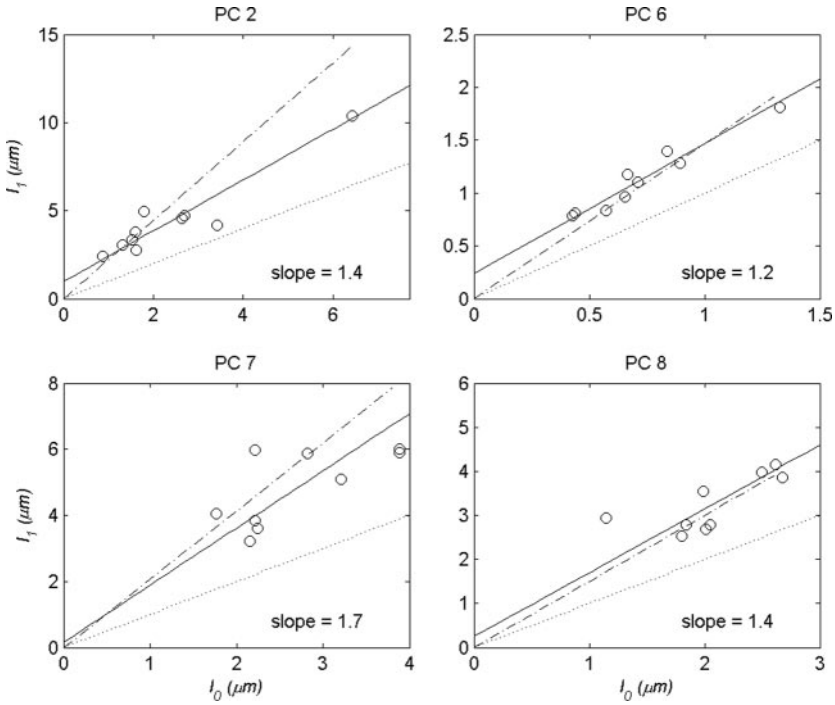

FIG. 14. I_1 vs. I_0 after PC adaptation. Conventions as in Fig. 13.

greater, suggesting some degree of multiplicativity. However, if adaptation effects are at least in part multiplicative, the slope should bear some relationship to the unadapted I_1/I_0 ratio. In other words, if there is a multiplicative component to adaptation, large initial I_1/I_0 ratios should result in large dI_1/dI_0 slopes. However, the *right panels* of Fig. 15 show that there is no relationship between dI_1/dI_0 and the initial I_1/I_0. Note, however, that because of the narrow range of unadapted I_1/I_0 ratios, this apparent independence should be interpreted with caution for PC afferents.

DISCUSSION

Comparing psychophysics and neurophysiology

EFFECTS OF ADAPTING AMPLITUDE. Prolonged suprathreshold vibratory stimulation was found to result in a reversible decrement in afferent sensitivity. Afferent thresholds increased systematically as the intensity of the adapting stimulus increased, which matches results from psychophysical studies showing declining vibratory sensitivity with increasing vibratory intensity (Berglund and Berglund 1970; Gescheider and

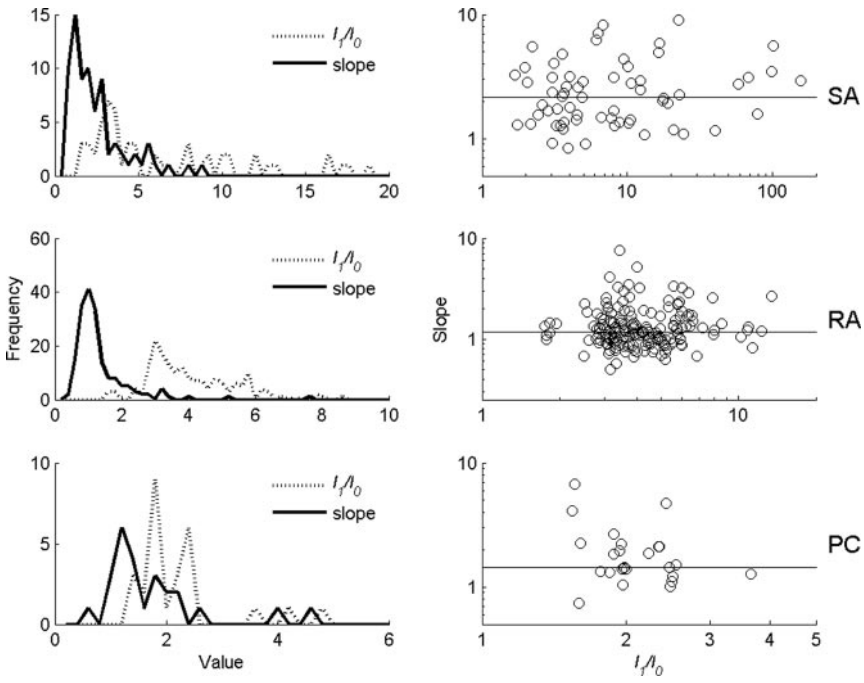

FIG. 15. Slope of adapted I_1 vs. I_0 and corresponding unadapted I_1/I_0 ratios. Each observation was derived from a single experimental run. Additive hypothesis predicts slope to be 1 regardless of unadapted I_1/I_0 ratio. Multiplicative hypothesis predicts slope to be equal to unadapted I_1/I_0 ratio. For RA afferents, slope is around unity regardless of I_1/I_0. For SA1 and PC afferents, slopes are intermediate between multiplicativity and additivity, although the mode for both types of afferents is near 1. That slopes were independent of I_1/I_0 for all afferents further weakens the multiplicative hypothesis.

Wright 1969; Gescheider et al. 1979; Hollins et al. 1991; Verrillo and Gescheider 1977). In psychophysical experiments studying the effects of adaptation on the detection of low-frequency stimuli, the slope of the function relating threshold shift to adapting amplitude ranged from 0.48 to 0.65 dB/dB (Gescheider et al. 1979; Hollins et al. 1991; Verrillo and Gescheider 1977). On the other hand, when the perception of the test stimulus was mediated by the Pacinian system, the slope was somewhat shallower at ~0.4 dB/dB (Gescheider et al. 1979).

In this study, the median slopes of the functions relating shifts in I_0 to adapting intensity—converted to decibels for the sake of comparison with psychophysical data—were 0.94 (0.5–1.1) and 0.50 (0.30–1.43) dB/dB for RA and PC afferents, respectively. Increasing the amplitude of the adaptor thus seems to have a greater effect on RA sensitivity than on psychophysical thresholds in the flutter frequency range (mediated at the sensory periphery by RA afferents). Similarly, PC afferents, less susceptible to adaptation than their RA counterparts, exhibited a sensitivity to adaptation commensurate with, but somewhat greater than, that observed when measuring psychophysical thresholds at high frequencies (mediated at the periphery by PC afferents).

At first glance, it seems paradoxical that the sensory periphery is more susceptible to vibratory adaptation than is the sensory system as a whole. This seeming discrepancy can be attributed to differences in the structure of the two types of experiments: psychophysical and neurophysiological. Specifically, in two of the three psychophysical experiments used in the comparison, the test intervals (when thresholds were actually measured and no adapting stimulus was present) were substantially longer than were their counterparts in these experiments (10 s in Hollins et al. 1990 and 30 s in Verrillo and Gescheider 1977 vs. 1 s in this study). Cutaneous afferents therefore had considerable time to recover during the test interval, given the rate at which afferents recover from vibratory adaptation (Leung et al. 2005). In the third set of psychophysical experiments (Gescheider et al. 1979), test intervals were short (1.5 s) and interleaved with adapting intervals (1 s) after presentation of an initial adaptor (lasting 10 min). However, the adapting stimulus was on only 40% of the time in the period during which thresholds were measured compared with 75% in this study.[2] The overall efficacy of the adaptor in the study of Gescheider et al. (1979) was therefore reduced relative to that in this experiment (Fig. 2). Differences in the temporal structure of the psychophysical and neurophysiological experiments thus account for the differences in the slopes relating threshold shift to adapting amplitude. Greater shifts in psychophysical thresholds would likely be observed if adaptation was measured with a procedure that more nearly matched the procedure used in this neurophysiological study.

EFFECTS OF ADAPTING FREQUENCY. In psychophysical studies, the effects of adapting frequency on sensory adaptation have been accounted for in terms of the frequency characteristics of a set of mechanoreceptive channels, each associated with a distinct population of mechanoreceptors. The adapting effects of a stimulus at a given frequency on a specific sensory channel have been thought to depend on its ability to excite that particular channel (Capraro et al., 1979; Gescheider et al. 1979; Hahn 1968a; Hollins et al. 1990; Verrillo and Gescheider 1977). For instance, the PC channel is relatively insensitive to low-frequency stimuli but highly sensitive to high-frequency stimuli. Accordingly, low-frequency stimuli adapt this channel only at high amplitudes, whereas high-frequency stimuli affect its sensitivity even at low amplitudes.

In this study, the adapting efficacy of stimuli that differed in frequency but were equated in amplitude was uncorrelated (even anticorrelated in the case of SA1 and RA fibers) with their effective amplitude, i.e., their amplitude relative to threshold. Although RA thresholds increased across the range of adapting frequencies used in this study (Fig. 3), high-frequency adaptors produced greater threshold shifts than low-frequency adaptors (Fig. 9). Similarly, although the Pacinian frequency characteristic is U-shaped, PC threshold shifts also increased systematically with adapting frequency (when other stimulus parameters were held constant). It thus seems that vibratory frequency has an effect on adaption beyond its effectiveness in activating the afferents.

The effects of frequency *per se* have, however, not been studied systematically in psychophysical studies (aside from attempts to isolate either RA or PC channels). When the effect of adaptation on RA-mediated thresholds using a 10-Hz test stimulus was measured using two adapting frequencies (10 and 50 Hz), it was found that the 50-Hz adaptor produced more adaptation than the 10-Hz adaptor, despite the fact that they were both set to the same sensation level (Hollins et al. 1990, 1991). Thus, the frequency of the adapting stimulus had an effect beyond that predicted from the spectral sensitivity of the channel.[3] More psychophysical experiments are required to elucidate the effects of adapting frequency on thresholds while controlling for their effective amplitudes.

In summary, the following observations can be made regarding the relationship between psychophysical adaptation and afferent adaptation. *1*) The slopes of the functions relating threshold shift to adapting intensity tend to be lower for psychophysical thresholds than for RA and PC afferents, although these differences may be caused by differences in the adaptation paradigm. *2*) Behaviorally, the effects of adapting frequency have been explained in terms of the spectral sensitivity profiles of the relevant sensory channels. In contrast, the frequency-dependence of adapting efficacy was uncorrelated (or even anticorrelated) with the spectral sensitivity of the mechanoreceptive afferents.

Neural mechanisms

There are, a priori, two hypotheses as to the neural mechanisms of vibratory adaptation in primary afferents. On the one hand, adaptation may be caused by a decrease in the effect of mechanical deformation on the conductance of the mechanosensitive ion channels that underlie transduction. This transducer gain hypothesis predicts a progressive depression in the

[2] Note that the effects of the 10-min initial adaptor on afferent sensitivity would have largely dissipated after 20-30 s (Leung et al. 2005).

[3] Note that equating two stimuli for subjective intensity does not ensure that they equally stimulate a given mechanoreceptive channel as the subjective intensity is a complex function of the neural activity evoked in the three main mechanoreceptive channels (Hollins and Roy 1996).

generator potentials elicited by an unchanging stimulus.[4] On the other hand, an increase in mechanical thresholds may be caused by an increase in spiking threshold. According to this hypothesis, the transducer mechanism is unaffected and stimulus-evoked receptor potentials remain stable over time, but a greater receptor potential is required to evoke an action potential. These hypotheses are, of course, not mutually exclusive.

To examine the predictions of these two hypotheses, we invoked a simple integrate-and-fire model of mechanotransduction, in the spirit of Freeman and Johnson (1982a). In this model, which accurately describes the vibratory stimulus–response relationship in primary afferents, spiking thresholds rise temporarily after an action potential and then return exponentially to their resting levels; furthermore, resting membrane time constants are very short (1–2 ms).[5] For the sake of simplicity, the function relating conductance to stimulus intensity is assumed to be linear with a slope determined by the transduction gain. The magnitude of the depolarization elicited on each stimulus cycle is then proportional to the receptor's gain. Let T be the spiking threshold of the afferent at rest, ΔT the residual increment in spiking threshold on a stimulus cycle after a cycle on which a spike was produced, and k the transducer gain. Because there is no residual threshold shift when the afferent has not yet produced an action potential, the (mechanical) absolute threshold is proportional to the spiking threshold and inversely proportional to the transducer gain. Because ΔT is approximately constant from cycle to cycle when the stimulus is entrained, the (mechanical) entrainment threshold is approximately proportional to $(T + \Delta T)$ and inversely proportional to the transducer gain. So

$$I_0 \propto \frac{T}{k} \tag{1}$$

$$I_1 \propto \frac{T + \Delta T}{k} \tag{2}$$

We can now examine predictions from the transducer gain and threshold hypotheses as to the relative effect of adaptation on I_0 and I_1. The increments in I_0 and I_1 produced by attenuating the transducer gain by a factor of a are given by

$$dI_0 \propto \frac{aT}{k} - \frac{T}{k} = \frac{(a-1)T}{k} = (a-1)I_0 \tag{3}$$

$$dI_1 \propto \frac{a(T+\Delta T)}{k} - \frac{T+\Delta T}{k} = \frac{(a-1)(T+\Delta T)}{k} = (a-1)I_1 \tag{4}$$

such that

$$\frac{dI_1}{dI_0} = \frac{I_1}{I_0} \tag{5}$$

As the transducer gain decreases, the increase in I_1 relative to that in I_0 is equal to the unadapted ratio of I_1 to I_0.

Another possibility is that adaptation acts on the spiking threshold by causing an increase in the resting spiking threshold T, by causing an increase in the residual refractory threshold elevation, ΔT, or both. Suppose T increases by b, and ΔT increases by c (note that I_0 is independent of ΔT). The increments in absolute and entrainment threshold are then given by

$$dI_0 \propto \frac{T+b}{k} - \frac{T}{k} = \frac{b}{k} \tag{6}$$

$$dI_1 \propto \frac{T+b+\Delta T+c}{k} - \frac{T+\Delta T}{k} = \frac{b+c}{k} \tag{7}$$

so that

$$\frac{dI_1}{dI_0} = 1 + \frac{c}{b} \tag{8}$$

Thus, if the resting threshold increases but the residual refractoriness does not (i.e., $b > 0$, $c = 0$), an increase in threshold causes an equal increment in I_0 and I_1, and $dI_1/dI_0 = 1$. In this case, the effect of adaptation is purely additive. On the other hand, if both the resting threshold, T, and the residual refractoriness, ΔT, increase with adaptation, the slope of the function relating I_1 to I_0 will be >1. In this case, the effect of adaptation is intermediate between additivity and multiplicativity. The degree of multiplicativity is a function of the increase in residual refractoriness relative to that in threshold (i.e., of c/b).

We have seen that the effect of prolonged vibratory stimulation on RA responsivity is to produce an equal increment in I_0 and I_1 (see Figs. 4, 6, 8, 10, and 13). Adaptation in this case is an unambiguously additive phenomenon, suggesting that it stems from an increase in the resting spiking threshold but not in the residual threshold elevation during the relative refractory period ($b > 0$, $c = 0$). On the other hand, SA1 afferents have a (geometric) mean dI_1/dI_0 ratio close to 2.0 (Fig. 14), which suggests a mechanism in which adaptation has the same effect on T and ΔT ($b = c$). The PC data (Fig. 14) also suggest elevations of both T and ΔT, but the number of observations is too small to draw a reliable conclusion.

The possibility remains that adaptation results from an increase in threshold accompanied by a decrease in transduction gain. In that case (and to the extent that *Eqs.* 1–8 are accurate), the effects of gain and threshold shift on threshold elevation would be given by

$$dI_0 = (a-1)I_0 + ab/k \tag{9}$$

$$dI_1 = (a-1)I_1 + a(b+c)/k \tag{10}$$

It is difficult to see a dependence of a, b, and c on the adapting amplitude that would result in the linear relationships between I_0, I_1 and adapting amplitude shown in Figs. 5–7. Likewise, it is difficult to see how the linear relationships shown in Figs. 12–14 could arise from the predicted relationship between the adapted I_1 and I_0

$$I_1 = I_0 + \frac{a(\Delta T + c)}{k} \tag{11}$$

unless either a or c was independent of the adapting amplitude. If, on the other hand, $a = 1$ and b and/or c was proportional to the adapting amplitude, *Eqs. 6* and *7* predict the linear relationships shown in Figs. 5–7 and 12–14.

[4] A related hypothesis is that the ions that flow through mechanosensitive channels become depleted during intense vibratory stimulation. This hypothesis makes predictions analogous to those of the transducer gain hypothesis.

[5] The rapid leak rate of the receptor membrane is a departure from a previous model of mechanoreception (Freeman and Johnson 1982a,b), as is the inclusion of a spike-induced threshold shift. However, these features have been validated experimentally (F. J. Looft, K. O. Johnson, and S. S. Hsiao, unpublished observations).

Biophysical mechanisms

For all three classes of afferents, the shift in threshold was found to be independent of the firing rate evoked by the adapting stimulus. Adaptation thus seems to depend on events occurring at the transduction site rather than at the spike initiation site. The critical event is likely transduction itself. Mechanoelectrical transducer channels have been found to be permeable to more than one cation (Diamond et al. 1958; Takeda et al. 2003). We speculate that one of these ions, probably calcium in SA1 and RA afferents, accumulates in the receptor during prolonged vibratory stimulation. The calcium buildup might cause a gradual increase in spiking threshold and/or relative refractoriness or, in PC afferents, a decrease in transduction gain (Loewenstein and Cohen 1959). Because the mechanically gated conductance increases with stimulus amplitude, calcium influx increases as the amplitude of the adapting stimulus increases. Furthermore, because there are more depolarizing phases per unit time as stimulus frequency increases, calcium influx also increases as the frequency of the adapting stimulus increases. Thus, the amplitude- and frequency-dependence of calcium influx or some other molecule can readily account for the dependence of threshold shift on the amplitude and frequency of the adapting stimulus.

The increase in spiking threshold that, we propose, underlies adaptation, at least in SA1 and RA afferents, may stem from a mechanism such as a calcium-gated potassium conductance ($I_{K(CA)}$) (Sah 1996). According to this hypothesis, the influx of calcium and the resulting increase in potassium conductance would result in a hyperpolarization of the resting receptor membrane. Such a hyperpolarization is functionally equivalent to an increase in spiking threshold: in both cases, a greater depolarization is required to reach threshold and produce an action potential. The $I_{K(CA)}$ hypothesis is supported by the fact that *1*) mechano-electrical transducer (MET) channels have been found to be permeable to calcium in Merkel disks (Tazaki and Suzuki 1998) and possibly Meissner corpuscles (Suzuki et al. 2003) and *2*) MET channels and calcium-gated potassium channels have been found to be colocalized and functionally linked in mechanically sensitive cells (Erxleben 1993).

Summary and conclusions

In this study, we developed a method to track afferent sensitivity as it changes over time. With this method, we showed for the first time that prolonged suprathreshold vibratory stimulation can produce a substantial desensitization of SA1, RA, and, to a lesser extent, PC afferents. The degree of adaptation increases linearly with the amplitude of the adaptor when test and adapting frequencies are held constant. Threshold shift also increases with adapting frequency when adapting amplitude is held constant. Furthermore, threshold shift seems to be independent of the firing rate evoked in the afferent by the adapting stimulus. All of these findings are consistent with an adaptation mechanism based on elevation of the spiking threshold because of (probably) calcium entry through mechanosensitive ion channels.

APPENDIX

In the range of stimulus amplitudes between I_0 and I_1, the relationship between firing rate and stimulus amplitude is nearly linear (Johnson 1974). If thresholds remain constant, I_0 and I_1 can be estimated by presenting stimuli whose amplitudes fall within this range and extrapolating the resulting (linear) rate-intensity function to amplitudes that yield firing rates of 0 and 1 impulses per cycle (for I_0 and I_1, respectively). Recovering I_0 and I_1 is not as straightforward when they are changing during adaptation and recovery.

A tracking algorithm was therefore developed to estimate I_0 and I_1 as they change over time. The algorithm generates test amplitude values for the next trial expected to evoke afferent firing rates between 0.2 and 0.8 impulses per cycle (ipc), a range within which responses optimally convey information about afferent sensitivity. The tracking algorithm was founded on three assumptions: *1*) the relationship between firing rate and stimulus amplitude is linear for amplitudes between I_0 and I_1 (Johnson 1974); *2*) the shifts in I_0 and I_1 between trials $n - 2$ and n are approximately twice those between trials $n - 2$ and $n - 1$; and *3*) the shifts in I_0 and I_1 are assumed equal. This assumption—reasonable for small threshold shifts—was used only to calculate the value of the test amplitude for the next trial in step 1. It was not used to generate estimates for I_0 and I_1; in step 2, the changes in I_0 and I_1 were assumed to be different and were calculated independently of one another.

List of variables

$f(n)$:	firing rate on the n^{th} trial (in impulses per cycle)
$f_d(n)$:	target (desired) firing rate on the n^{th} trial
$I(n)$:	test amplitude on n^{th} trial (predicted to yield $f_d(n)$)
$I_{f_d}(n-2)$:	test amplitude that would have yielded $f_d(n)$ on trial $n - 2$ (calculated post hoc)
$I_0(n)$:	actual absolute threshold on trial n
$I_1(n)$:	actual entrainment threshold on trial n
$I'_0(n)$:	estimate of $I_0(n)$
$I'_1(n)$:	estimate of $I_1(n)$
dI:	estimate of the change in I_0 and I_1 between trials $n - 1$ and n *(step 1)*
dI_0:	estimate of the change in I_0 between trials $n - 1$ and n *(step 2)*
dI_1:	estimate of the change in I_1 between trials $n - 1$ and n *(step 2)*

At the nth step, the quantities that are known and can be used to move forward are *1*) the stimulus intensities used in the current and previous steps, $I(j), j = 1 \ldots n$, 2) the firing rates evoked at those stimulus intensities $f(j), j = 1 \ldots n$, and *3*) estimates of the absolute and entrainment thresholds at all the previous steps, $I_0(j)$ and $I_1(j)$, j = 1. . .n − 1.

The algorithm comprises two steps. The object of the first step is to predict the stimulus intensity at the next step, $I(n + 1)$, that will produce a firing rate between 0.2 and 0.8 ipc [i.e., within $(I_0\ I_1)$]. The object of the second step is to update the estimates of I_0 and I_1: once the firing rate, $f(n + 1)$, evoked by $I(n + 1)$ is known, $I_0(n)$ and $I_1(n)$ can be estimated.

Step 1: predicting the appropriate intensity, I(n + 1), for the next step

The intensity required to produce a target rate $f_d(n + 1)$ between 0 and 1 is

$$I(n+1) = [1 - f_d(n+1)] \times I_0(n+1) + f_d(n+1) \times I_1(n+1) \quad (12)$$

The problem is, of course, that I_0 and I_1 for the next step, $n + 1$, are not known. The last estimates of I_0 and I_1 are $I'_0(n - 1)$ and $I'_1(n - 1)$ (estimates of I_0 and I_1 are designated I'_0 and I'_1). A linear approximation, which we invoke only in step 1, is that I_0 and I_1 increase by the same amount, dI, between test intervals. If we knew dI, we could calculate the appropriate intensity by invoking assumption 2 and

substituting $I'_0(n-1) + 2 \times dI$ and $I'_1(n-1) + 2 \times dI$ for $I_0(n+1)$ and $I_1(n+1)$ in *Eq. 12*

$$I(n+1) = [1 - f_d(n+1)] \times I'_0(n-1) + f_d(n+1) \times I'_1(n-1) + 2 \times dI \quad (13)$$

Note that the quantity $[1 - f_d(n+1)] \times I'_0(n-1) + f_d(n+1) \times I'_1(n-1)$ is the stimulus intensity that would have yielded the firing rate $f_d(n+1)$ on trial $n-1$. $I'_0(n-1)$ and $I'_1(n-1)$ are known, so an estimate of dI is needed. The question is, what dI produces the firing rate $f(n)$ evoked by the stimulus of amplitude $I(n)$ presented on the current trial. Using the approximation as above, except $I'_0(n) = I'_0(n-1) + dI$ and $I'_1(n) = I'_1(n-1) + dI$, we obtain

$$I(n) = [1 - f(n)] \times I'_0(n-1) + f(n) \times I'_1(n-1) + dI \quad (14)$$

and therefore

$$dI = I(n) - [1 - f(n)] \times I'_0(n-1) - f(n) \times I'_1(n-1) \quad (15)$$

which can be substituted back into *Eq. 13* to obtain $I(n+1)$.

Step 2: estimating $I_0(n)$ and $I_1(n)$

After a stimulus of intensity $I(n+1)$ computed with *Eqs. 13* and *15*, is presented on trial $n+1$ to evoke $f(n+1)$, I_0 and I_1 for the nth trial can be estimated. We use the same logic of linear approximation as in step 1, except that I_0 and I_1 are allowed to change by different amounts, dI_0 and dI_1, between intervals $n-1$ and n and between intervals n and $n+1$. We now have two (I,f) response pairs, $[I(n),f(n)]$ and $[I(n+1), f(n+1)]$ with which to solve two simultaneous equations for dI_0 and dI_1, namely

$$I(n) = [1 - f(n)]) \times [I'_0(n-1) + dI_0] + f(n) \times [I'_1(n-1) + dI_1] \quad (16)$$

$$I(n+1) = [1 - f(n+1)] \times [I'_0(n-1) + 2 \times dI_0] + f(n+1) \times [I'_1(n-1) + 2 \times dI_1] \quad (17)$$

Rewriting these in more conventional form for simultaneous equations (so that dI_0 and dI_1 are on the left side)

$$[1 - f(n)] \times dI_0 + f(n) \times dI_1 = I(n) - [1 - f(n)] \times I'_0(n-1) - f(n) \times I'_1(n-1) \quad (18)$$

$$2 \times [1 - f(n+1)] \times dI_0 + 2 \times f(n+1) \times dI_1 = I(n+1) - [1 - f(n+1)] \times I'_0(n-1) - f(n+1) \times I'_1(n-1) \quad (19)$$

Equations 18 and *19* can be solved easily for dI_0 and dI_1 if the equations are not degenerate. The determinant is

$$d = 2 \times \{[1 - f(n)] \times f(n+1) - f(n) \times [1 - f(n+1)]\} \quad (20)$$

where it can be seen that the determinant is zero or near zero when $f(n)$ and $f(n+1)$ are equal or comparable. Thus the method requires that successive stimuli be selected so that $f(n)$ and $f(n+1)$ are different. Accordingly, the target responses, $f_d(n)$, alternated between higher and lower values [within (0.2 0.8)] on successive trials (e.g., 0.2, 0.5, 0.3, 0.6, 0.4, 0.7, 0.5, 0.8, etc.). Even more disparate target rates (e.g., 0.1 and 0.9) could have been used to calculate $I(n+1)$, but they too often result $I(n+1)$ values less than $I_0(n+1)$ or greater than $I_1(n+1)$, which evoke responses that violate the linearity assumption.

Because the tracking algorithm requires initial estimates of the afferent's I_0 and I_1 values, measurements were performed in the preadaptation period to generate these by presenting stimuli at various intensities and measuring the evoked firing rates. The test amplitude for the first trial of the adaptation period was set midway between $I_0(0)$ and $I_1(0)$, the initial estimates of the absolute and entrainment thresholds. After that, the test amplitudes were determined by the tracking algorithm.

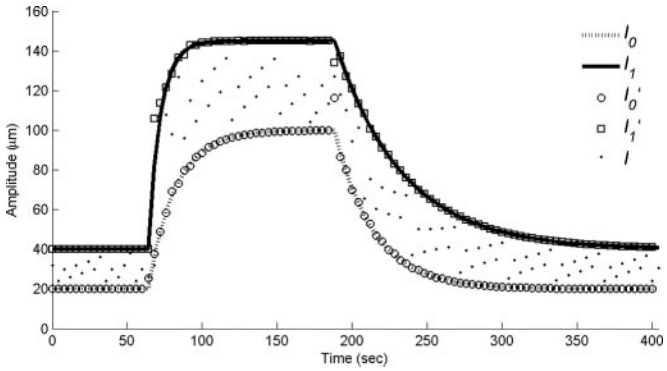

FIG. 16. Algorithm performance on simulated data. Simulated thresholds (I_0 and I_1) were programmed to be constant during the preadaptation period, to increase exponentially during the adaptation period, and to decline exponentially to preadaptation levels during recovery period. Time constants and adaptation shifts were derived from an actual RA afferent (RA 17). The tracking algorithm generated test amplitudes, I, and estimated thresholds, I_0 and I_1; based on simulated firing rates. Dashed and solid lines represent hypothetical I_0 and I_1 values as they vary over the course of adaptation and recovery, respectively. Open circles and squares represent the algorithm's estimates of those I_0 and I_1 values at 4-s intervals, respectively. Dots represent test amplitudes generated by the algorithm at each step.

The algorithm was tested on simulated data to assess its ability to recover changing thresholds. Because the algorithm assumes a linear increase in threshold from step n to $n+2$ (assumption 2), it can easily recover thresholds if they change by a constant amount. On the other hand, the algorithm is maximally challenged if the slope at which thresholds change is itself constantly changing, as is the case if threshold are shifting along exponential time-courses. Therefore simulated values of I_O and I_I were programmed to increase and then decrease exponentially (Fig. 16). The tracking algorithm was provided with an estimate of the initial thresholds, and, on each trial, with the firing rate, $f(n)$, evoked by the test amplitude, $I(n)$, provided by the algorithm. Invoking assumption 1 (linearity), the firing rate elicited on trial n was given by

$$f(n) = \frac{I(n) - I_0(n)}{I_1(n) - I_0(n)} \quad (21)$$

where $I_0(n)$ and $I_1(n)$ are the actual (simulated) thresholds on trial n. These simulations showed that the algorithm was able to track these thresholds even as they changed rapidly. Figure 16 shows the results of a typical simulation. Similar results were obtained when the tracking algorithm was used to recover thresholds that followed other mathematical functions of time (logarithmic, linear, exponential with positive exponents, etc.).

ACKNOWLEDGMENTS

We thank A. Sripati and T. Yoshioka for insightful discussion. We are also indebted to K. Ledoux, M. Hollins, and J. Craig for careful reading of the manuscript.

GRANTS

This work was supported by National Institute of Neurological Disorders and Stroke Grants NS-18787, NS-38034, and NS-34086.

REFERENCES

Berglund U and Berglund B. Adaption and recovery in vibrotactile perception. *Percept Mot Skills* 30: 843–853, 1970.

Capraro AJ, Verrillo RT, and Zwislocki JJ. Psychophysical evidence for a triplex system of cutaneous mechanoreception. *Sens Processes* 3: 334–352, 1979.

Chubbuck JG. Small motion biological stimulator. *Johns Hopkins APL Tech Digest* 5: 18–23, 1966.

Delemos KA and Hollins M. Adaptation-induced enhancement of vibrotactile amplitude discrimination: the role of adapting frequency. *J Acoust Soc Am* 99: 508–516, 1996.

Diamond J, Gray JAB, and Inman DR. The depression of the receptor potential in Pacinian corpuscles. *J Physiol* 141: 117–131, 1958.

Erxleben CF. Calcium influx through stretch-activated cation channels mediates adaptation by potassium current activation. *Neuroreport* 4: 616–618, 1993.

Freeman AW and Johnson KO. A model accounting for effects of vibratory amplitude on responses of cutaneous mechanoreceptors in macaque monkey. *J Physiol* 323: 43–64, 1982a.

Freeman AW and Johnson KO. Cutaneous mechanoreceptors in macaque monkey: temporal discharge patterns evoked by vibration, and a receptor model. *J Physiol* 323: 21–41, 1982b.

Gescheider GA, Frisina RD, and Verrillo RT. Selective adaptation of vibrotactile thresholds. *Sens Processes* 3: 37–48, 1979.

Gescheider GA and Wright JH. Effects of sensory adaptation on the form of the psychophysical magnitude function for cutaneous vibration. *J Exp Psychol* 77: 308–313, 1968.

Gescheider GA and Wright JH. Effects of vibrotactile adaptation on the perception of stimuli of varied intensity. *J Exp Psychol* 81: 449–453, 1969.

Goble AK and Hollins M. Vibrotactile adaptation enhances amplitude discrimination. *J Acoust Soc Am* 93: 418–424, 1993.

Goble AK and Hollins M. Vibrotactile adaptation enhances frequency discrimination. *J Acoust Soc Am* 96: 771–780, 1994.

Hahn JF. Vibrotactile adaptation and recovery measured by two methods. *J Exp Psychol* 71: 655–658, 1966.

Hahn JF. Low-frequency vibrotactile adaptation. *J Exp Psychol* 78: 655–659, 1968a.

Hahn JF. Tactile adaptation. In: *The Skin Senses,* edited by Kenshalo DR. Springfield, IL: Charles C Thomas, 1968b, p. 322–330.

Hollins M, Delemos KA, and Goble AK. Vibrotactile adaptation on the face. *Percept Psychophys* 49: 21–30, 1991.

Hollins M, Delemos KA, and Goble AK. Vibrotactile adaptation of the RA system: a psychophysical analysis. In: *Somesthesis and the Neurobiology of the Somatosensory Cortex,* edited by Franzén O, Johansson RS, and Terenius L., Basel: Birkhäuser, 1996, p. 101–111.

Hollins M, Goble AK, Whitsel BL, and Tommerdahl M. Time course and action spectrum of vibrotactile adaptation. *Somatosens Mot Res* 7: 205–221, 1990.

Hollins M and Roy EA. Perceived intensity of vibrotactile stimuli: the role of mechanoreceptive channels. *Somatosens Mot Res* 13: 273–286, 1996.

Johnson KO. Reconstruction of population response to a vibratory stimulus in quickly adapting mechanoreceptive afferent fiber population innervating glabrous skin of the monkey. *J Neurophysiol* 37: 48–72, 1974.

Keidel WD, Keidel UO, and Wigand ME. Adaptation: loss or gain of sensory information? In: *Sensory Communication,* edited by Rosenblith WA. Cambridge: MIT Press, 1961, p. 319–338.

Lee CJ and Whitsel BL. Mechanisms underlying somatosensory cortical dynamics: I. In vivo studies. *Cereb Cortex* 2: 81–106, 1992.

Lee CJ, Whitsel BL, and Tommerdahl M. Mechanisms underlying somatosensory cortical dynamics: II. In vitro studies. *Cereb Cortex* 2: 107–133, 1992.

Leung YY, Bensmaïa SJ, Hsaio SS, and Johnson KO. Time-course of vibratory adaplation and recovery in cutaneous mechanoreceptive afferents. *J Neurophysiol* 94: 3038–3046, 2005.

Loewenstein WR and Cohen S II. Post-tetanic potentiation and depression of generator potential in a single non-myelinated nerve ending. *J Gen Physiol* 43: 347–376, 1959.

O'Mara S, Rowe MJ, and Tarvin RP. Neural mechanisms in vibrotactile adaptation. *J Neurophysiol* 59: 607–622, 1988.

Sah P. Ca2+-activated K+ currents in neurons: types, physiological roles and modulation. *Trends Neurosci* 19: 150–154, 1996.

Suzuki M, Oyama Y, Kusano E, Mizuno A, Irao A, and Ookawara S. Localization of mechanosensitive channel TRPV4 in mouse skin. *Neurosci Lett* 353: 189–192, 2003.

Takeda M, Nishikawa T, Sato S, Aiyama S, and Matsumoto S. Effects of gadolinium and tetrodotoxin on the response of slowly adapting type I mechanoreceptors to mechanical stimulation in frog dorsal skin. *J Peripher Nerv Syst* 8: 271–281, 2003.

Talbot WH, Darian-Smith I, Kornhuber HH, and Mountcastle VB. The sense of flutter-vibration: comparison of the human capacity with response patterns of mechanoreceptive afferents from the monkey hand. *J Neurophysiol* 31: 301–334, 1968.

Tazaki M and Suzuki T. Calcium inflow of hamster Merkel cells in response to hyposmotic stimulation indicate a stretch activated ion channel. *Neurosci Lett* 243: 69–72, 1998.

Verrillo RT and Gescheider GA. Effect of prior stimulation on vibrotactile thresholds. *Sens Processes* 1: 292–300, 1977.

Whitsel BL, Kelly EF, Delemos KA, Xu M, and Quibrera PM. Stability of rapidly adapting afferent entrainment vs responsivity. *Somatosens Mot Res* 17: 13–31, 2000.

Whitsel BL, Kelly EF, Quibrera M, Tommerdahl M, Li Y, Favorov OV, Xu M, and Metz CB. Time-dependence of SI RA neuron response to cutaneous flutter stimulation. *Somatosens Mot Res* 20: 45–69, 2003.